MODELING OF NONEQUILIBRIUM PLASMA ASSISTED COMBUSTION

Tropina A.A.

National Automobile and Highway University, Kharkov, Ukraine

The different discharges action on the combustion process is one of the effective ways of the combustion process control. Over the past decades a lot of the experimental data has been accumulated, which is devoted to the discharges influence on ignition and combustion processes. This is directly related to the widespread use of discharges in the modern plasma technologies. Generally, we can divide the plasma assisted combustion in two groups, depending on the mechanisms of the discharge influence on the ignition or combustion process. According to the thermal mechanism, the discharge leads to equilibrium or near equilibrium low-temperature plasma creation. In this case, the thermal heating of the gas causes an increase of the thermal dissociation rate and, consequently, an initiation of the combustion process. One example of the thermal mechanism realization is the spark or arc discharge ignition. This type of discharges is characterized by a falling current–voltage characteristic, a relatively low voltage drop across electrode layers (less than 100 A) and high currents (up to tens of kA) and, more importantly, a very high gas temperature. Main characteristics and numerical aspects of such equilibrium plasma modeling are analyzed in the review [1].

According to the nonthermal mechanism, the discharge energy mainly goes to the electron heating with the minimal gas heating, and at some conditions the additional energy transfer channel is realized through the vibration of molecules levels and then through the vibrational–translational relaxation. In this case the nonequilibrium plasma is formed. One of the main advantages of such plasma is an achievement of the chemical reactions selectivity and possibility to manage by an electron temperature and electron number density distribution at the low power budget. A great number of the experimental data devoted to the investigations of different nonequilibrium gas discharges is available in the literature. A review of the most recent experimental data is presented in [2], where the author has analyzed a nonequilibrium plasma influence on combustion and ignition processes. It should be noted that the presented experimental data confirm an energy perspective of the chemical reaction artificial initiation by the low temperature nonequilibrium plasma. As a consequence, most modern applications of nonequilibrium plasma assisted combustion have focused on the aerospace [3–6]. Recent works have demonstrated a capability of the air–fuel mixture ignition and combustion control by nonequilibrium discharges in supersonic flows by means of the flame front stabilization with a significant increase in the flame velocity compared with arc and spark discharges [7,8]. The most popular ways of the nonequilibrium plasma creation are corona, microwave, dielectric barrier discharge and the nanosecond repetitive pulsed

(NRP) discharge. The last one can be viewed as one of the leading technologies for plasma assisted combustion and as a reliable ignition source under different operation conditions [9,10]. Among the works devoted to the practical application of a nonequilibrium plasma, for example, in internal combustion engines, the works [11,12] can be noted.

Most of the experimental studies devoted to the investigation of kinetic mechanisms of the ignition process by a nonequilibrium plasma of the nanosecond pulsed discharge were carried out at low pressure conditions. For example, in [13] the authors have presented results of time-dependent measurements of oxygen atom and nitric oxide density in air, air/methane and air/ethylene mixtures. At atmospheric pressure conditions only limited data of species measurements are available, because of the experiment complexity. The results of the measurements of $N_2(C^3\Pi_u)$ and $N_2(B^3\Pi)$ metastables density for the nanosecond repetitively pulsed discharge in nitrogen and air preheated at 1000 K are presented in [14]. For methane–air mixture no direct measurements of species concentrations are available in the literature, only in [15] the authors have presented the experimental data of the vibrational and translational temperature distribution.

A lack of the experimental data is a main reason for the mathematical modeling to become a main tool in the predictions of nonequilibriun plasma assisted combustion. We can underline the following main physical mechanisms of the ignition and combustion processes assisted by a nonequilibrium plasma of the NRP discharge: 1) the ignition delay time decrease caused by the generation of electronically and vibrationally excited particles, 2) the laminar flame velocity increase caused by the additional generation of radicals and by the possible influence of the vibrational temperature on the combustion reaction rate; 3) a possible additional transfer of momentum, which causes a generation of the small-scale turbulence in the discharge zone; 4) the influence of energy stored in the vibrational degrees of freedom on the minimum ignition energy and on the combustion process; 5) a possible change of the ignition kinetic mechanism; 6) change of transport properties of the reaction medium.

First two mechanisms as well as the last two ones are discussed in details in [16–18]. This paper is devoted to such phenomenon as the minimum ignition energy in the case of nonequilibrium plasma ignition. The minimum ignition energy is often described as the amount of energy required to heat the gas (fuel and oxidizer) from its initial state to the adiabatic flame temperature or as the energy which is sufficient to drive the flame kernel beyond the critical radius. It is experimentally proved that the minimum ignition energy (the MIE) depends on many parameters such as a mixture composition, pressure, the hydrodynamic characteristics as well as the way of ignition. Phenomenon of the MIE is well studied in the case of spark ignition. The main properties of the minimum ignition energy in this case can be summarized as follows: the MIE depends on the electric circuit properties, discharge duration and on the inter-electrode gap

width [19]. According to one of the last papers devoted to the MIE phenomenon the transition between different combustion modes can be determined as the change of the character of the MIE dependence on the velocity pulsations level [20].

At the same time the data about the MIE measurements and calculations in the case of other discharges ignition are not very numerous. For example, for laser ignition according to the data presented in [21] the experimental values of the minimum ignition energy are higher that the analogous ones for spark ignition. It has been shown in [21] that the values of the MIE depend on energy and duration of a laser pulse and on the laser beam wavelength and lens focal length. In the case of the nanosecond repetitively pulsed discharge ignition the only one paper [22] regarding the experimental measurements of the MIE was found in the literature. In [22] the experimental values of the MIE were presented in the case of propane–air mixture ignition and these values were in an order higher than the MIE values for spark ignition. It is quite clear that the plasma volume created in the experiments is much higher than the minimal volume needed for ignition. Thus the question of the MIE phenomenon for nonequilibrium plasma ignition is still open.

1. Formulation of the problem. Let's introduce as characteristic values of the velocity, distance, time, pressure, density, concentration of neutral particles, concentration of charged components, electric current density, induction of the magnetic field and electron temperature such variables as υ_0, d_0, $t_0 = \frac{d_0}{\upsilon_0}$, p_0, $\rho_0 = \frac{p_0 Y_0}{R T_0 m_0}$, Y_0, n_0, $j_0 = \frac{B_0 c}{d_0 \mu}$, $B_0 = \frac{E_0 c}{\upsilon_0}$, T_e^0. Let's choose as the characteristic scales of reaction mixture properties their values at temperature T_0 and pressure p_0, i.e. $\rho_0, \lambda_0, \eta_0, c_p^0, D_e^0, D_i^0$ and as the characteristic scales of the mixture temperature and enthalpy $\theta = \frac{T - T_0}{T_i - T_0}$, $\tilde{H} = \frac{H - H_0}{H_i - H_0}$, where T_i, H_i is the mixture temperature and enthalpy in the ignition moment. After that the main equations describing plasma assisted combustion can be written in the following nondimensional form

$$\frac{\partial \bar{\upsilon}}{\partial t} + (\bar{\upsilon} \cdot \nabla)\bar{\upsilon} = -Eu \nabla p + \frac{1}{\rho Re}\left(\nabla\left(2\tilde{\eta}\upsilon_{ik} + \frac{1}{3}div\bar{\upsilon}\,\delta_{ik}\right)\right) + \frac{1}{\rho}\left(G_q \bar{E} + Al \cdot \bar{j} \times \bar{B}\right), \quad (1)$$

$$\frac{\partial \rho}{\partial t} + div\left(\rho \bar{\upsilon}\right) = 0, \quad (2)$$

$$\frac{\partial n_i}{\partial t}+(\bar{\upsilon}\cdot\nabla)n_i=\frac{\beta}{\rho\cdot Sc_e\cdot Re}\operatorname{div}(\rho\tilde{D}_i^i\nabla n_i)-$$
$$-(-1)^{i-1}\frac{\beta}{\rho Re_{э'}}\operatorname{div}\left(\frac{\tilde{D}_i^i n_i\rho\bar{E}}{\theta+\theta_0}\right)+\sum_{j=1}^{N}Da_j\varphi_j(\theta)\cdot\tilde{W}(Y_i,n_i,n_e) \quad , \quad (3)$$

$$\frac{\partial n_e}{\partial t}+(\bar{\upsilon}\cdot\nabla)n_e=\frac{1}{\rho\cdot Sc_e\cdot Re}\operatorname{div}(\rho\tilde{D}_e\nabla n_e+\rho k_T\frac{\nabla\theta}{\theta+\theta_0})+$$
$$+\frac{1}{\rho Re_e}\operatorname{div}\left(\frac{n_e\rho\tilde{D}_e\bar{E}}{\theta+\theta_0}\right)+Da_e\varphi_e(\theta)\cdot\tilde{W}_e(Y_i,n_i,n_e) \quad , \quad (4)$$

$$\frac{\partial Y_i}{\partial t}+(\bar{\upsilon}\cdot\nabla Y_i)=\frac{1}{\rho\cdot Sc_i\cdot Re}\operatorname{div}(\rho\tilde{D}_i\nabla Y_i)+$$
$$+\sum_{j=1}^{n}Da_j\varphi_j(\theta)\cdot\tilde{W}(Y_i,n_i,n_e)\ \ i=\overline{1,n} \quad , \quad (5)$$

$$\operatorname{div}(\tilde{\varepsilon}\bar{E})=\xi(\sum_{i=1}^{N}n_i-n_e)\,, \quad (6)$$

$$\frac{\partial}{\partial t}(n_e\theta_e)+\frac{\partial}{\partial x_i}\left(\frac{5}{2}\upsilon_i n_e\theta_e\right)=(Re\cdot Pr_e)^{-1}\nabla\lambda_e\cdot\nabla\theta_e+G_{de}\dot{j}\cdot\bar{E}-$$
$$-G_{Te}\nu_{eff}(\theta_e-\varsigma_e\theta)-G_{e\_V}Q_{e-V}-G_eQ_e \quad , \quad (7)$$

$$c_p^*\rho\left(\frac{\partial\theta}{\partial t}+\bar{\upsilon}\cdot\nabla\theta\right)=(Pr\cdot Re)^{-1}\nabla\lambda^*\cdot\nabla\theta+G_T\nu_{eff}(\varsigma_e^{-1}\theta_e-\theta)+$$
$$+G_{VT}\rho\frac{\varepsilon_\upsilon(\theta_\upsilon)-\varepsilon_0(\theta)}{\tau_{VT}}+\frac{1}{Re}\operatorname{div}\left(\rho\sum_{i=1}^{n}(\frac{1}{Sc_i}h_i\tilde{D}_i\nabla Y_i\right)+ \quad , \quad (8)$$
$$+\sum_{j=1}^{r}\rho^2Da_j\varphi_j(\theta,\theta_e,\theta_V)\cdot h_j\cdot\tilde{W}(Y_j,n_j,n_e)$$

$$\frac{d\varepsilon_\upsilon}{dt}=(Sc_\varepsilon\cdot Re)^{-1}\nabla\cdot\rho D_h\nabla\varepsilon_\upsilon-G_{VT\varepsilon}\rho\frac{\varepsilon_\upsilon(\theta_\upsilon)-\varepsilon_0(\theta)}{\tau_{VT}}+G_{\varepsilon-V}Q_{e-V}\,, \quad (9)$$

$$p=\rho(\theta+\theta_0)\sum_{i=1}^{n}\frac{Y_i}{m_i}\,, \quad (10)$$

$$\bar{j}=Re_m(\sigma\bar{E}+\sigma\bar{\upsilon}\times\bar{B})\,, \quad (11)$$

where n_i, n_e, Y_i are the concentrations of ionic components, electrons and neutral particles including electronically and vibrationally excited metastables, $\theta, \theta_e, \varepsilon_\upsilon$ are the translational, electronic and vibrational temperature,

D_e, D_i^j, D_i are the diffusion coefficients of electrons, ions and neutral particles, k_T is the thermal diffusion coefficient of electrons, $\widetilde{W}(Y_j, n_j, n_e)$ is the reaction rate constant with the exponential term modified using a conversion of Frank–Kamenetskii.

The nondimensional parameters of the system (1)–(11) are as follows

$$\mathrm{Re} = \frac{\rho_0 \upsilon_0 d_0}{\eta_0},\ G_q = \frac{e n_0 E_0 d_0}{\rho_0 \upsilon_0^2},\ \alpha_j = \frac{RT_i}{U_j},\ \mathrm{Re_m} = \frac{\sigma_0 d_0 \mu \upsilon_0}{c},\ \mathrm{Sc_i} = \frac{\eta_0}{\rho_0 D_i},$$

$$I_d = \frac{\sigma_0 E_0^2 d_0}{\rho_0 \upsilon_0 (H_i - H_0)},\ \ \mathrm{Al} = \frac{j_0 B_0 d_0}{\rho_0 \upsilon_0^2},\ \theta_i = \frac{T_i}{T_i - T_0},\ \ G_e = \frac{2Q_e^0 d_0}{3 n_{e0} k_B T_{e0} \upsilon_0},$$

$$\mathrm{Da_j} = k_j \exp\left(-\frac{1}{\alpha_j}\right),\ \varphi_j(\theta) = \exp\left(-\frac{\theta - 1}{\alpha_j \theta_i}\right),\ \mathrm{Re_e} = \frac{E_0 e D_e}{\upsilon_0 k_B (T_i - T_0)},$$

$$\mathrm{Sc_e} = \frac{\eta_0}{\rho_0 D_e},\ \xi = \frac{4\pi e n_0 d_0}{\varepsilon_0 E_0},\ \beta = \frac{D_{i0}}{D_{e0}},\ \mathrm{Pr} = \frac{\eta (H_i - H_0)}{\lambda (T_i - T_0)},\ \theta_0 = \frac{T_0}{T_i - T_0},$$

$$\mathrm{Pr_e} = \frac{3\eta_0 n_e^0 k_B}{2\rho \lambda_e^0},\ \varsigma_e = \frac{T_e^0 - T_0}{T_e^0},\ G_{e-V} = \frac{2Q_{e-V}^0 d_0}{3 n_{e0} k_B T_{e0} \upsilon_0},\ G_{d\varepsilon} = \frac{j_0 E_0 d_0}{\varepsilon_0 \upsilon_0},$$

$$G_{Te} = \frac{\nu_{eff}^0 x_0 \delta_{eff}}{n_{e0} \upsilon_0},\ \ G_{VT} = \frac{c_p^0 d_0 \varepsilon_0(T_0) R}{\rho_0 \upsilon_0 (T_i - T_0) \tau_{VT}^0 k_B},\ G_{de} = \frac{2 j_0 E_0 d_0}{3 n_{e0} k_B T_{e0} \upsilon_0},$$

$$G_T = \frac{3\nu_{eff}^0 d_0 \delta_{eff}}{2\upsilon_0 c_p^0 \rho_0},\ \mathrm{Sc}_\varepsilon = \frac{\eta_0 k_B}{\rho_0 D_h R},\ \ G_{VT\varepsilon} = \frac{\rho_0 R d_0}{\upsilon_0 \tau_{VT}^0 k_B}, G_{\varepsilon - V} = \frac{Q_{e-V}^0 d_0}{\varepsilon_0 \upsilon_0},$$

$$\varsigma_V = \frac{T_V - T_0}{T_0},\ Q_{e-V} = \alpha_V G_{d\varepsilon} \bar{j} \cdot \bar{E},$$

where Q_{e-V} is the term describing the exchange processes between electronic and vibrational energies; τ_{VT} is the vibrational–translational relaxation time; D_h is the diffusion coefficient of excited molecules; $\varepsilon_\upsilon(T_\upsilon)$, $\varepsilon_0(T)$ are the nonequilibrium and equilibrium vibrational energy; $\delta_{eff} = \frac{2m_e}{m_0}$ is the effective coefficient of electron scattering by molecules; ν_{eff} is the cross-section of elastic collisions of electrons; α_V is the fraction of the electron energy transferred into the excitation of vibrational levels; D_V is the vibrational thermal conductivity; Q_e is the energy lost by electrons on the excitation of electronic and vibrational levels and on the ionization.

The system of equations (1)–(11) includes transport equations that describe the conservation of mass, momentum and chemical species such as electrons, ions and neutral particles in the case of low Mach number approximation. It also includes the equation for the electric field strength and Ohm's law (Maxwell equations at the absence of the external magnetic field) and transport equations for translational, electronic and vibrational temperatures on the basis of three-temperature model in the mode approximation described in details in [23].

The dimensionless parameters $G_{e-V}, G_{Te}, G_{\varepsilon}, G_e$ determine, respectively, the ratio of the heat transfer in exchange processes between electronic and vibrational energies (G_{e-V}), of the heat transfer in the process of elastic collisions of electrons with molecules (G_{Te}, G_T), of the heat transfer in the process of vibrational–translational exchange and thermal excitation of vibrational, electronic levels and ionization G_e to the convective heat transfer. Parameters $G_{VT\varepsilon}, G_{\varepsilon-V}, G_{d\varepsilon}$ determine the ratio of the following terms to the convective transfer of vibrational energy: the vibrational energy loss in the vibrational–translational relaxation process, the vibrational energy loss in the process of exchange between the electronic and vibrational energies; the energy produced in the process of vibrational excitation. The mixture specific heat and thermal conductivity c_p^*, λ^* are calculated taking into account the contribution of vibrational excitation.

In the case of nonequilibrium plasma assisted combustion $G_q << 1$, $\varsigma_e < 1$, $\varsigma_V > 1$, $Al << 1$ and reaction rate constants are the functions of three temperatures $\varphi_j = \varphi_j(\theta, \theta_e, \theta_V)$. As the nanosecond pulse width is very short compared with the characteristic times of diffusion and convection in the first stage the nonequilibrium plasma composition can be calculated neglecting by the diffusion and convection processes, on the basis of equations (3)–(9) in one-dimensional geometry as in [16]. In the second stage we consider the laminar flame propagation problem based on equations (1)–(5), (8)–(9) at $G_T = G_{\varepsilon-V} = 0$ to calculate the minimum ignition energy using as initial conditions the nonequilibrium plasma composition formed after the nanosecond repetitively pulsed discharge and the distribution of translational and vibrational temperatures.

Additional parameter of the problem was the radius of a nonequilibrium plasma spot and the minimum ignition energy was calculated by the minimization of this radius. The energy added to the mixture by the nonequlibrium plasma spot was calculated as the difference between volume–averaged internal energy of the mixture before and after plasma input. Main neutral components of the mixture were taken according to the GRI 3.0 mechanism [24], the plasma components were as follows $O_2(a^1\Delta)$, $O_2(b^1\Sigma)$,

$O_2(c^1\Sigma)$, $O(^3P)$, O^-, O_3^-, NO_2^-, $N_2(x^1\Sigma,\nu)$, NO^+, O^+, O_2^+, e^-.

Concentrations of the electronically excited states of nitrogen and some other plasma components compared with the model in [16] were neglected due to their short life time and a low content in the fuel–air mixture ignited by the nanosecond pulsed discharge. Transport properties of the fuel–air mixture with plasma components were determined by the following equations of the molecular theory of gases [25]:

$$(\lambda_t)_{ij} = 1989{,}1\cdot 10^{-7}\left[T(M_i + M_j)/(2M_iM_j)\right]^{1/2}/\Omega_{i,j}^{(1,1)} \quad ,$$

$$(\eta)_{ij} = 266{,}93\cdot 10^{-7}\left[2T\cdot M_iM_j/(M_i + M_j)\right]^{1/2}/\Omega_{i,j}^{(2,2)} \quad ,$$

$$(D)_{ij} = 0{,}002628\left[T^3(M_i + M_j)/(2M_iM_j)\right]^{1/2}/p\Omega_{i,j}^{(1,1)} \quad ,$$

where M_i is the mass of mixture component, $\Omega_{i,j}^{(1,1)}$ is the diffusion collision integral, $\Omega_{i,j}^{(2,2)}$ is the viscosity collision integral, η is the dynamic viscosity.

For the air neutral species collisions the data presented in [26] were used. For the methane–air neutral species collisions Lenard–Jones potential was used. Eiken corrections to mixture transport properties connected with excited particles were neglected due to low temperature ($T < 6000$ K). Collisions between electrons and neutral components as well as between electrons and positive and negative ions were neglected due to low concentrations of electrons. For collisions between charged and neutral species the polarizability method was used [27] and values of thermal conductivities, diffusion and viscosity coefficients were determined through the component polarizability α by the following

$$(\lambda_t)_{ij} = 5{,}37\cdot 10^{-7}T\left[(M_i + M_j)/(2M_iM_j)\right]^{1/2}/z/\alpha^{1/2} \quad ,$$

$$(\eta)_{ij} = 1{,}02\cdot 10^{-7}T\left[(M_iM_j)/(M_i + M_j)\right]^{1/2}/z/\alpha^{1/2} \quad ,$$

$$(D)_{ij} = 6{,}177\cdot 10^{-6}T^2\left[(M_i + M_j)/(2M_iM_j)\right]^{1/2}/z/p/\alpha^{1/2} \quad ,$$

where z is the charge number.

As an ignition criterion the maximum heat release rate was chosen. The minimum ignition energy was evaluated according to the relation

$$E_{min} = \frac{4}{3}\pi\cdot r_{min}^3\rho_0 c_p(T_{ad} - T_0) \, , \qquad (12)$$

where T_{ad} is the adiabatic flame temperature, r_{min} is the characteristic dimension of the preheated layer, ρ_0, T_0 are the initial density and temperature of the mixture.

The problem was solved in two-dimensional geometry; the calculation domain was a rectangle 50 mm×50 mm. The domain is composed of triangular cells, the grid cell size is 0,005 mm. The equations (1)–(5), (8)–(9) were

discretized by using the finite volume method. Central differences were employed for the evaluation of the diffusion terms, for the evaluation of the convective ones the second order upwind differences were used. Discretized equations were solved in a coupled manner by the implicit method of second order in time. It was assumed that the convergence of the time-marching procedure was achieved if the residuals were below 10^{-5}. On the boundaries the concentrations of plasma components are assumed zero, $T = T_V = 300^{\circ}K$ and $Y_{fuel} = Y^0_{fuel}$, $Y_{O_2} = Y^0_{O_2}$, where $Y^0_{fuel}, Y^0_{O_2}$ are the initial concentrations of the fuel (methane or ethylene) and oxidizer in the reaction mixture depending on the mixture equivalence ratio Φ.

2. Calculation results. The main questions to be answered are how the pulse width of the NRP discharge, the reduced electric field of the discharge, the energy stored in the vibrational degrees of freedoms and the nonequilibrium plasma composition influence on the minimum ignition energy. In the first stage the computational results of the minimum ignition energy in the case of the nanosecond repetitively pulsed discharge ignition were compared with that for thermal ignition at atmospheric pressure conditions. It was obtained that for the all considered cases the minimum ignition energy for nonthermal ignition is higher than the analogous values for the case of thermal ignition. As the characteristic dimension of the preheated layer r_{min} in (12) the plasma spot radius was used.

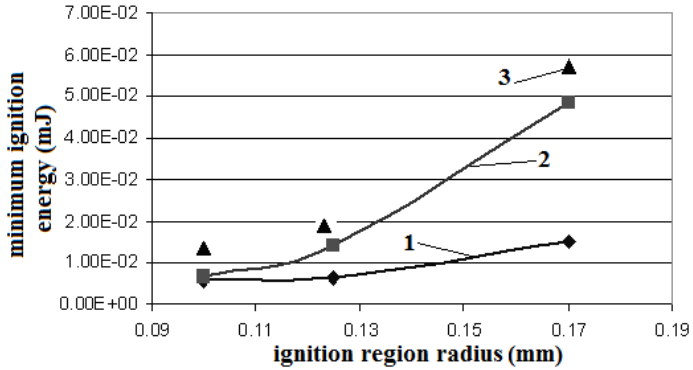

Fig. 1. The minimum ignition energy as a function of the initial kernel radius: 1 − thermal ignition [28], 2 − nonequilibrium plasma ignition, 3 − nonequilibrium plasma ignition without vibrational excitation

In Fig.1 we have compared the calculation results of the MIE for the lean methane–air mixture at ignition time less than $t = 10^{-7}$ s presented in [28] and the calculation results of the MIE for the lean methane–air mixture with the same

equivalence ratio $\Phi = 0{,}65$ but ignited by a nonequilibrium plasma of the NRP discharge (pulse width 20 ns, maximum voltage 20 kV). The initial kernel radius was the same for thermal and nonequilibrium plasma ignition. For ignition by nonequilibrium plasma two cases of initial conditions after the discharge were considered such as the nonequilibrium plasma ignition with the effect of vibrational excitation on the reaction rates (case 2) and the nonequilibrium plasma ignition without the effect of vibrational excitation (case 3). It is seen from Fig.1 that the vibrational excitation leads to a lower MIE (about 17%). It should be also noted that for small values of the initial kernel radius ($r \cong 0.1$ mm) the minimum ignition energy for the lean methane–air mixture ignited by nonthermal plasma is very close the MIE for the methane–air mixture ignited by thermal plasma. The increase of the initial ignition radius causes the increase of the MIE for both thermal and nonequilibrium plasma ignition and enlarges the difference between them.

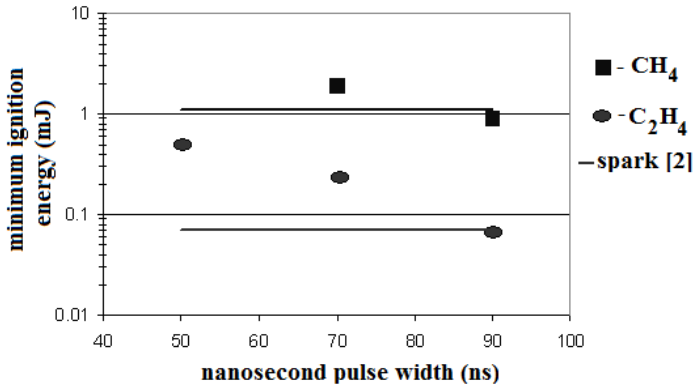

Fig. 2. The minimum ignition energy as a function of pulse width

At the same time if we use as the characteristic dimension of the preheated layer r_{min} the quenching distance, the calculated values of the MIE are very close to the experimental values of the minimum ignition energy for spark ignition [19] for a longer nanosecond pulse width (Fig.2). The calculated results presented in Fig.2 correspond to the case of stoichiometric CH_4 –air and C_2H_4 – air mixtures ignition by the NRP discharge with maximum voltage of the pulse $U = 20$ kV. As it was previously mentioned for a short nanosecond pulse width the calculated values of the MIE are higher than the analogous ones for spark ignition. This tendency is observed for both methane–air and ethylene–air mixtures.

It should be noted that the calculated data presented in Fig.2 correspond to the case of ignition by the NRP discharge with the different pulse width but at the same maximum voltage of the discharge. The decrease of the MIE with a

pulse width at the same discharge voltage is connected with the increase of the input discharge energy; and as a consequence the part of energy going to the radicals' formation in addition to heating is increased. The both cases cause the minimum ignition energy decrease.

The simulation also shows that if we decrease the nanosecond pulse width at the same discharge energy by increasing the maximum discharge voltage the minimum ignition energy is decreased (Fig.3). For the lean methane–air mixture this reduction of the MIE is minimal, but for the stoichiometric mixture this effect is much more pronounced and the reduction reaches approximately 50%. This result implies that the effect by shortening of the nanosecond pulse width to achieve gains in the minimal ignition energy for the case of the lean methane–air mixture ignition is very limited.

If we compare the calculated values of the MIE for the lean and stoichiometric methane–air mixture (Fig.3), it is seen that the minimum ignition energy is minimal for the lean fuel–air mixture as for a case of spark ignition. At the same time the modeling results have shown that the influence of the vibrational –translational relaxation into the initial flame kernel formation and the influence of mixture heating due to the vibrational –translational relaxation process on the MIE are negligible. The minimum ignition energy is more sensitive to the initial temperature and plasma composition formed by the nanosecond pulsed discharge and decreases with the increase of the maximum reduced electric field of the discharge E/N (Fig.4).

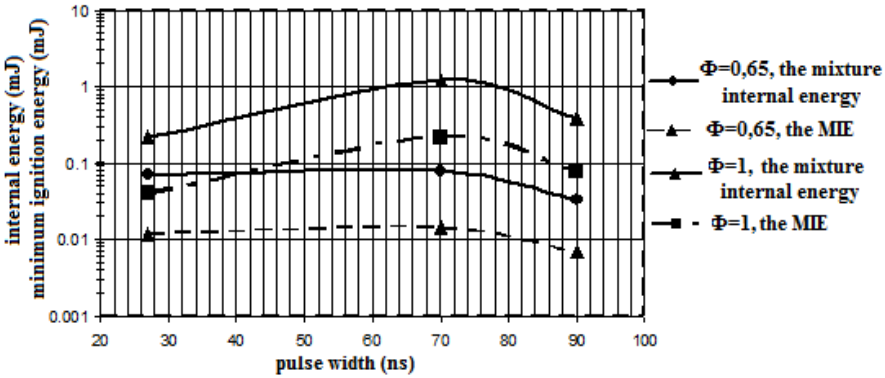

Fig.3. The mixture internal energy and the MIE as a function of pulse width

It is seen from Fig.3 that for the all considered cases the minimum ignition energy defined according to (12) does not exceed 15–20% of the difference between the internal energies of the mixture before and after nonequilibrium plasma input.

In summary two different ways of the minimum ignition energy decrease exist in the case of ignition by the nanosecond repetitively pulsed discharge.

More effective way of the MIE decrease for the lean methane–air mixture is the increase of the nanosecond pulse width. The main mechanism of the minimum ignition energy reduction in this case is the mixture heating. For the stoichiometric methane–air mixture more effective decrease of the MIE can be obtained by the nanosecond pulse width decrease. The main mechanism of the MIE reduction in this case is the additional generation of fuel dissociation products due to the increased reduced electric field.

Comparing the obtained results of the minimum ignition energy with the data of the ignition delay time presented in [16], it should be noted that for ignition of the lean methane–air mixture the NRP discharge is more effective in the ignition delay time decrease. On the other hand, for ignition of the stoichiometric mixture the discharge is more effective in reducing the minimum ignition energy by varying the pulse width.

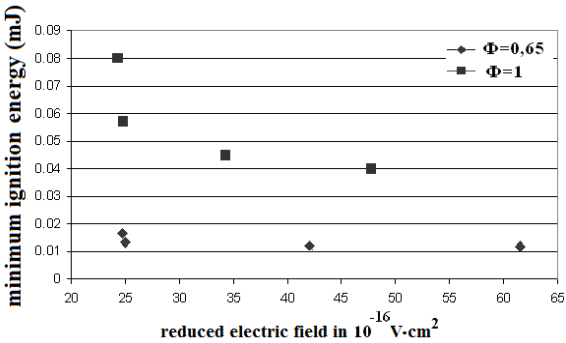

Fig. 4. The minimum ignition energy dependence on the maximum reduced electric field of the discharge

3. Conclusions. The calculated data of the minimum ignition energy in a case of ignition by the nonequilibrium plasma as a basis for the improvement and modernization of ignition sources using the nanosecond pulsed discharge have been presented.

REFERENCES

1. Gleizes A., Gonzales J. J., Freton P. Thermal plasma modeling // J. Phys. D: Appl. Phys. – 2005.– v.38.– R.153–183.
2. Starikovskaya S. M. Plasma assisted ignition and combustion // J. Phys. D: Appl. Phys. – 2006.– v. 39.– R265–299.
3. Klimov A., Bityrin V., Nikitin A. et al. Non-Premixed Plasma Assisted Combustion in High-Speed Flow // Proc 43nd AIAA Aerospace Sciences Meeting and Exhibit. – Reno, 2005.– Paper AIAA–2005–599.

4. Esakov I. I., Grachev L. P., Khodataev K. V., Vinogradov V. A., Van Wie D.M. Efficiency of propane–air mixture combustion assisted by deeply undercritical MW discharge in cold high-speed airflow // Proc. 44th AIAAA Aerospace Sciences Meeting and Exhibit. – Nevada, USA. – 2006. – Paper AIAA–2006–1212.
5. Anikin N. V., Mintoussov E. I., Pancheshnyj S. V., Roupassov D. V., Sych V. E., Starikovskij A. Yu. Nonequilibrium plasmas and its applications for combustion and hypersonic flow control // Proc. 41nd AIAA Aerospace Sciences Meeting and Exhibit. – Nevada, USA . – 2003. – Paper AIAA–2003–1053.
6. Klimov A., Bityrin V., Moralev I., Tolkunov B., Nikitin A., Velichko A., Bilera I. Non-Premixed Plasma Assisted Combustion of Hydrocarbon fuel in High-Speed Airlow // Proc. 44nd AIAA Aerospace Sciences Meeting and Exhibit. – Nevada, USA . – 2006. – Paper AIAA–2006–617.
7. Leonov A. V., Yarantsev D. A., Napartovich A. P., Kochetov I. V. Plasma assisted ignition and flameholding in high-speed flow // Proc. 44th AIAAA Aerospace Sciences Meeting and Exhibit. – Nevada, USA. – 2006. – Paper AIAA–2006–563.
8. A.A. Nikipelov, A.E. Rakitin, I.B. Popov, G. Correale, A.Yu. Starikovskii. Plasmatrons powered by pulsed high voltage nanosecond discharge for ultra-lean flame stabilization // Proc. 49th AIAAA Aerospace Sciences Meeting and Exhibit. – Florida, USA. – 2011. – Paper AIAA–2011–1214.
9. Low G., Bao A., Nishihara M., Keshav S., Utkin Y. G., Adamovich I. V. Ignition of premixed hydrocarbon–air flow by repetitively pulsed, nanosecond pulse duration introduction plasma // Proc 44st AIAA Aerospace Sciences Meeting and Exhibit. – Nevada, USA . – 2006. – Paper AIAA–2006–1215.
10. Starikovskii A. Yu. Plasma supported combustion // Proc. of Comb. Inst. – 2005.– v.30. – P. 2405–2417.
11. Puchkarev V., Gundersen M. Energy efficient plasma processing of gaseous emission using a short pulse discharge // Appl. Phys. Lett. – 1997. – v.71(23). – P. 3364–3366.
12. Tropina A. A., Lenarduzzi L., Marasov S. V., Kuzmneko A. P. Comparative analysis of engine ignition systems // IEEE Trans. on Plasma Science. – 2009. – v. 37. – P. 2286–2292.
13. Uddi M., Jiang N., Adamovich I. V., Lempert W. R. Nitric oxide density measurements in air and air/fuel nanosecond pulse discharge by laser induced fluorescence// J. Phys.: Appl.Phys. – 2009. – v.42. – P. 075205–075223.
14. Stancu G. D., Kaddouri F., Lacoste D. A., Laux C. O. Atmospheric pressure plasma diagnostics by OES, CRDS and TALIF // J. Phys. D: Appl. Phys. – 2010. – v.43. – P. 124002–124012.
15. Messina D., Attal–Tretout B., Grisch F. Study of a non-equilibrium nanosecond discharge at atmospheric pressure using coherent anti-Stokes Raman skattering // Proc. of the Comb. Inst. – 2007. – Vol.31. – P. 825–832.

16. Tropina A.A., M. Uddi M., Ju Y. Non-equilibrium plasma influence on the the minimum ignition energy. Part 1: Discharge model // IEEE Trans. on Plasma Sci. − 2011. −Vol.39. − P.615– 623.
17. Kosarev I.N., Aleksandrov N.L., Kindysheva S.V., Starikovskaya S.M., Starikovskii A.Y. Kinetic mechanism of plasma–assisted ignition of hydrocarbons // J. Phys.D: Appl.Phys. – 2008. – Vol.41. – P.032002–032008.
18. Тропіна А.А. Mechanisms of ignition by the nanosecond pulsed discharge (in Russian)// Aerospace engineering and technology. − 2010. –Vol. 5(72). – С.64–70.
19. Eckhoff R.K. Explosion hazards in process industries. − Houston: Gulf Publishing Company, 2005. – 457 p.
20. Huang C.C., Shy S.S., Liu C.C., Yan Y.Y. A transition on the minimum ignition energy for lean turbulent methane combustion in flamelet and distributed regimes // Proc. of the Combustion Institute. −2007. − Vol.31. − P.1401–1409.
21. Phuoc T.X., White F.P. Laser–Induced spark ignition of CH_4/air mixtures // Combustion and flame. − 1999. − Vol.119. −P.203–216.
22. Pancheshnyi S., Lacoste D.A., Bourdon A., Laux C.O. Ignition of propane–air mixture by a sequence of nanosecond pulses // European Conf. for Aerospace Sciences (EUCASS), Moscow. − 2005. − N 5.12.05(3).
23. Tropina A.A. Modeling of nonequilibrium air plasma generation by transversal gas discharge // IEEE trans. on Plasma Science. – 2008. – Vol. 36, N 6. – P.2887–2891.
24. Smith G.P., Golden D.M., Frenklach M., Moriarty N.W., Eiteneer B., Goldenberg M., Bowman C.T., Hanson R.K., Song S., Gardiner W.C., Lissianski V.V., Qin Z. [Online]. Available. http://www.me.berkeley.edu/gri_mec.
25. Hirschfelder J., Curtiss C.F., Bird R.B.. Molecular theory of gases and liquids. − New York: Willey, 1966. − 1249 p.
26. Capitelli M., Gorse C., Longo S.. Collision integrals of high temperature air species // Journal of thermophysics and heat transfer. − 2000 . − Vol. 14. −P. 259– 268.
27. Handbook of chemistry and physics, 84th edition. − New York: CRC press, 2003–2004.
28. Frendi A., Sibulkin M. Dependence of the minimum ignition energy on ignition parameters // Combust. Sci. and Tech. – 1990. – Vol.73. – P. 395–413.